First-principles molecular dynamics of the initial oxidation of Si{001} by ozone

Christian K. Fink and Stephen J. Jenkins*
Department of Chemistry, University of Cambridge, Cambridge CB2 1EW, United Kingdom
(Received 18 July 2008; revised manuscript received 12 September 2008; published 6 November 2008)

Ozone has recently received considerable attention as an alternative oxidant in the low-temperature oxidation of silicon. Here, we use density-functional theory to elucidate the initial oxidation stages of O_3 on Si{001}. Ozone favors a barrierless dissociation with two surface reaction centers involving either the up (Si^u) or the down (Si^d) dimer atom of the buckled Si dimer. The Si^u site exhibits a strong steering effect which leads typically to partial dissociation, whereas Si^d initially interacts only weakly with the molecule, resulting sometimes in complete dissociation. We discuss the underlying electronic structure of the reaction, with particular emphasis on the spin evolution.

DOI: 10.1103/PhysRevB.78.195407 PACS number(s): 68.43.Bc, 34.35.+a, 81.65.Mq, 82.30.−b

I. INTRODUCTION

The Si/SiO_2 interface with its application in microelectronic industries is arguably one of the most important material interfaces. Its excellent interface characteristics, among many other desired properties, has turned silicon into the semiconducting material of first choice. The common growth technique is to use molecular oxygen at high temperatures (usually $>800\ ^\circ C$),[1,2] which faces, however, challenges in the sub-4-nm-thickness regime. In this ultrathin regime, the compositional and structural transition that occurs at around 1 nm thickness starts to play an important role.[3]

As an alternative, a low-temperature oxidation reduces the risk of inducing dopant migration and enables processing of temperature sensitive materials (e.g., low-temperature-poly-Si thin-film transistors). Among various approaches, advanced low-temperature oxidation methods include microwave plasma oxidation, xenon excimer lamp irradiation, and the high-concentration O_3 method.[3]

Ozone is more environmentally friendly than other oxidizing species such as N_2O and NO_2, since simply by heating it decomposes into molecular oxygen.[4] Compared to other radical oxygen species, O_3 can be generated in high concentrations, where molecules exhibit low kinetic energies in a thermal velocity distribution. This is a clear advantage over plasma oxidation techniques, which often cause sample damage due to highly energetic particle bombardment and exhibit only a low oxidation rate due to low radical flux.[5]

The first to study ozone for silicon oxidation was Chao *et al.*[6] who observed an increase in the oxidation rate. Kazor *et al.*[7] recognized the potential of ozone for low-temperature oxidation and with the development of high-purity ozone generators[4,5,8] a series of experiments have set out to characterize the Si/SiO_2 interface formed by the action of ozone. It was found that the interface exhibits less strain[9] and the notorious transition layer is reduced.[10] The ozone-grown oxide's device properties have also been tested for metal-oxide-semiconductor-field-effect transistor (MOS-FET) operations and improved reliability characteristics were observed.[11] Most recently it was reported that the silicon oxidation rate by ozone, in contrast to conventional molecular dioxygen, does not depend on the orientation of the Si crystal surface, which enabled the formation of a high-quality Si/SiO_2 interface even on polycrystalline silicon.[12]

The growth mode during the initial oxidation stage was found to proceed in accordance with Langmuir kinetics, which changed into linear kinetics at oxide thicknesses above 0.6 nm.[13] Regarding adsorption of O_3 onto clean silicon surfaces, little is known thus far. Bright features observed in scanning tunneling microscope (STM) studies following exposure of Si{001} to ozone were interpreted as individual O adatoms,[14,15] but whether each molecule deposits only a single adatom (partial dissociation) or three adatoms that subsequently diffuse (complete dissociation) remains obscure.

Despite the growing amount of experimental data, no theoretical study has been conducted yet (apart from our own recent work on the hydrogen-passivated surface[16]). The present paper aims at filling this gap by providing a detailed insight into the interaction of O_3 with a clean Si{001} surface from first-principles calculations. Here, we focus on the *initial* oxidation stage, which is expected to be distinct from other oxygen species. In contrast, the later oxidation stage (>0.6 nm) is expected to be governed by diffusion of atomic oxygen[17,18] and thus we expect the growth of the later SiO_2 film by ozone to be very similar to other oxygen radicals (e.g., atomic oxygen).

We begin by examining the possible reaction products and their energetics. Next we study intact adsorption structures of ozone and discuss their stability. Then we apply molecular-dynamics (MD) simulations to investigate the most probable reaction trajectories and finally we discuss the electronic structure to explain the observed reactions and relate our findings to experimental work, in particular to observed STM features.

II. METHODOLOGY

Figure 1 shows the side view of a relaxed Si{001} surface in its $p(2\times2)$ reconstruction. The top-layer silicon atoms form a dimer bond; in addition, charge transfer into one of the dimer silicon atoms creates an asymmetry, in which the upper Si-dimer atom (Si^u) is electron rich and the down Si-dimer atom (Si^d) is electron deficient. In a $p(2\times2)$ unit-cell dimers along the row alternate their tilt; whereas perpendicular to the row, the dimers are parallel.

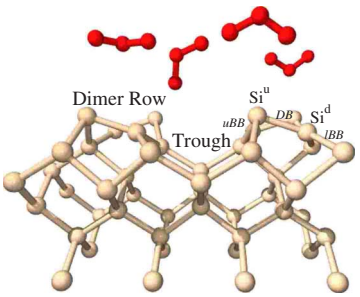

FIG. 1. (Color online) Side view of four ozone molecule orientations above a p(2×2) reconstructed Si{001} surface. Adsorption sites labeled accordingly: Si^d down Si-dimer atom, Si^u up Si-dimer atom, DB, lBB, and uBB.

The figure is annotated to highlight most likely adsorption sites during the initial oxidation process, including the up dimer atom (Si^u), the down dimer atom (Si^d), the dimer bond (DB), the lower backbond (lBB), and the upper backbond (uBB). This labeling will be used throughout the present paper.

We have also taken into consideration how the molecular orientation of the impinging O_3 molecule affects the reaction. This is indicated in Fig. 1 by showing the ozone molecule in various representative orientations considered in this work.

The results of all calculations presented here are based on density-functional theory (DFT) within the generalized-gradient approximation (GGA), using a plane-wave basis set in a periodic supercell arrangement.[19] The electron-electron exchange-correlation interactions were described by the Perdew-Wang (PW91) parametrization[20] and the electron-ion interactions were approximated by ultrasoft pseudopotentials as introduced by Vanderbilt.[21] A **k**-point sampling of the Brillouin zone based on the Monkhorst-Pack grid[22] was used [e.g., 2×2×1 grid for the p(2×2) cell].

The surface was modeled as a periodic slab, introducing an artificial periodicity normal to the surface. The (2×2) supercell consisted of six layers of four silicon atoms each with the bottom two layers fixed. In order to avoid any interslab interaction, a vacuum region of at least 10 Å was inserted and hydrogen atoms were added to passivate the dangling bonds of the bottom layer. A silicon bulk lattice constant of 5.38 Å was calculated separately and employed through fixed cell dimensions in all surface calculations. In the expansion of the wave functions we set the kinetic-energy cutoff at 340 eV. Bond lengths for O_2 and O_3 were calculated to be 1.23 and 1.28 Å, respectively, which are in good agreement with the experimental values of 1.21 and 1.29 Å. To optimize the structures we employed a quasi-Newton minimizer based on the Broyden-Fletcher-Goldfarb-Shanno (BFGS) algorithm.[23] The adsorbed molecule and the top layers of the slab were allowed to relax until residual forces were smaller than 0.05 eV/Å. Atomic charges are computed via a Mulliken population analysis by projecting the ground-state wave functions onto a basis consisting of *s*- and *p*-atomic orbitals.[24]

In addition, we have employed Born-Oppenheimer molecular dynamics to simulate surface reactions. We used an NVE ensemble, keeping the number of atoms, volume, and the total energy of the system constant, with an MD time step of 0.2 fs.[25] Spin polarization was found to influence the trajectories and was therefore included in all dynamic calculations.

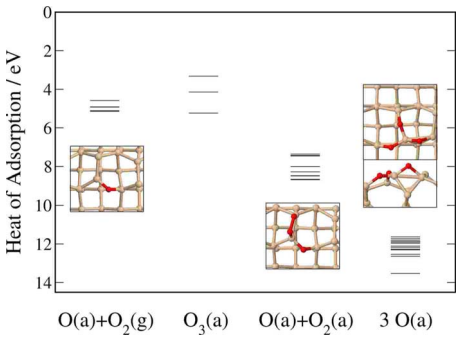

FIG. 2. (Color online) Heats of adsorption of ozone reaction products on a p(2×2) Si{001} surface. The most stable structure for each reaction group is shown from top view: a single O atom in lBB, O_2 adsorbed on DB with O atom in lBB, and three O atoms in DB, uBB, and the siloxane bridge (top and front view)

In the MD trajectories presented, all silicon atoms are initially at rest and the ozone molecule, which was placed in its rotational and vibrational ground state, approaches the surface with an initial velocity between 400–500 m/s (i.e., 4–5 Å/ps or 0.04–0.06 eV). This corresponds to the rms speed of an ensemble of ozone molecules at temperatures between 300 and 500 K. We have tested a range of higher and lower velocities for the impinging O_3 molecule and have also tested a surface where silicon atoms were assigned initial thermal velocities in the range of 300–500 K. Both tests revealed little qualitative difference from the results presented below.

III. RESULTS

A. Plausible reaction products

We start our investigation by studying possible reaction products and comparing their energetic stability. In order to do so, we have placed the ozone molecule in its gas phase geometry at various heights directly above different surface sites and performed a structure optimization. Each data point in Fig. 2 corresponds to the heat of adsorption from one of the resulting optimized structures. As reference point for the heat of adsorption, we took the sum of the energy of an isolated O_3 molecule and a clean silicon surface slab. A detailed analysis of all structures is beyond the scope of this study and, as we will see later, would add little to our quest to reveal the reaction pathway of ozone. Instead, we look at energy trends and describe the most stable structure for each species.

Optimized structures were grouped according to their final reaction product and we present them in order of increasing stability: (i) partial dissociation, where O adsorbs and O_2 desorbs; (ii) intact O_3 chemisorption which will be discussed in greater detail below; (iii) partial dissociation, where both O and O_2 adsorb; and (iv) complete dissociation into three

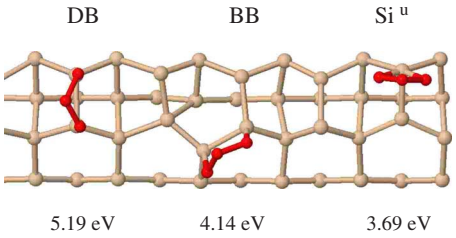

FIG. 3. (Color online) Chemisorbed O_3 structures on Si{001}. Adsorption sites: O_3 bound to dimer bond, back bond, and up Si-dimer atom.

adsorbed oxygen atoms. The energy spread within each of these reaction products highlights the role played by the adsorption sites. We have also looked at coverage effects by extending our simulation to a (4×4) unit cell. We find that due to structural relaxation a lower O coverage exhibits less local strain relative to the clean reconstructed surface, which results in a slightly higher heat of adsorption.[26] Since this effect is small compared to the absolute heat of adsorption, we concentrate our discussion on the (2×2) cell only. For a single O adatom we observe that the most stable adsorption site is the lBB, which is in agreement with previous DFT studies.[27] Upon partial dissociation into gas phase molecular O_2 and a single O atom incorporating the lBB, a heat of adsorption of 5.14 eV is released. Other adsorption sites, which play an important role in the ozone oxidation as MD simulations will show, include DB and Si^u, which release heats of adsorption of 5.09 and 4.19 eV, respectively.[28]

A partial dissociation where both atomic O and molecular O_2 stick to the surface is energetically more favorable and releases up to 8.66 eV. In the most stable structure O_2 encompasses the DB, while the O atom occupies the lBB of the same dimer. In our MD simulations later discussed, we will find this structure as a short-lived intermediate in the reaction leading to complete dissociation. Such a complete dissociation is the most exothermic reaction,[29] releasing a heat of up to 13.51 eV. In the most stable structure all three O atoms bind to the same Si-dimer atom by occupying the DB, uBB, and the siloxane bridge.[30,31]

Despite ozone's high reactivity, static calculations nevertheless reveal three intact chemisorbed structures on the surface. Ozone, as seen in Fig. 3, either bridges the DB and the BB (in this adsorption structure the dimer is horizontal) or adsorbs onto the up silicon atom (Si^u) and releases a heat of adsorption of 5.19, 4.14, or 3.69 eV, respectively. These energies are in the same order of magnitude as the partial dissociation of ozone into adsorbed O and desorbed O_2. Except for the Si^u chemisorption site, ozone induces the previously asymmetric Si dimer to become more symmetric.

To illustrate the change in surface and adsorbate electron distribution upon adsorption, we define the electron-density difference $\Delta\rho(\mathbf{r})$ as $\Delta\rho(\mathbf{r})=\rho_{O_3/Si}(\mathbf{r})-[\rho_{O_3}(\mathbf{r})+\rho_{Si}(\mathbf{r})]$, where $\rho_{O_3/Si}(\mathbf{r})$ represents the calculated electron density of ozone bound to the surface, $\rho_{O_3}(\mathbf{r})$ as the electron density of ozone with the surface removed, and $\rho_{Si}(\mathbf{r})$ of the surface with the adsorbate removed.

The most stable intact adsorption geometry is discussed in more detail in Fig. 4. The intramolecular O-O bond stretches

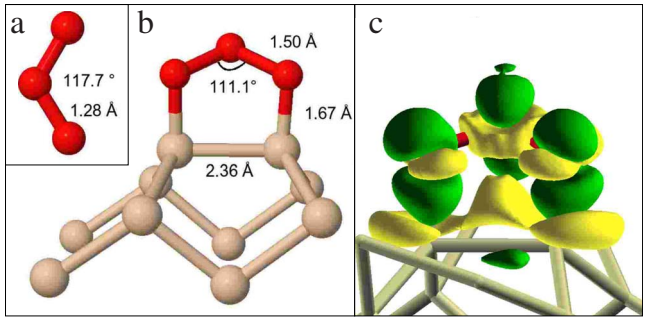

FIG. 4. (Color online) Most stable chemisorbed O_3 structure on Si{001}. (a) Geometry of gas phase O_3; (b) geometry and (c) electron-density difference plot of O_3 bound to dimer bond; [isosurface threshold at $0.05e$ $Å^{-3}$, green (dark): electron accumulation; yellow (light): electron depletion].

from 1.28 Å in the gas phase (a) by more than 15% to 1.50 Å upon adsorption (b). To understand the origin of this large strain on the intramolecular oxygen-oxygen bonds we have investigated the electron-density difference $\Delta\rho(\mathbf{r})$. A visualization of $\Delta\rho(\mathbf{r})$ [Fig. 4(c)] reveals electron depletion spread around the binding Si-dimer atoms, the encompassed Si-Si dimer bond, and ozone's in-plane molecular orbitals (MOs). Electron accumulation is localized in ozone's out-of-plane MOs. Calculations of gas phase ozone relate these depleted and accumulated regions to the highest occupied MO [(HOMO) bonding] and the lowest unoccupied MO [(LUMO) antibonding], respectively. It is expected that this electron redistribution from a bonding into an antibonding MO weakens the intramolecular oxygen-oxygen bonds. To quantify the electron transfer we have performed a Mulliken population analysis and find that the interacting silicon dimer atoms have become strongly positive, each donating around $0.63e$ with respect to a neutral Si atom; whereas the ozone molecule receives a total charge of $-1.16e$, of which $-0.35e$ are transferred to the central O atom and $-0.41e$ each to the terminal O atoms. This large electron accumulation in ozone's antibonding LUMO helps to explain the increase in the O-O bond lengths by more than 15% upon adsorption and suggests that intact ozone adsorption is unstable with respect to dissociation.

B. Molecular dynamics

It is clear from our static geometry optimizations that ozone is highly reactive at the Si{001} surface, many different reaction products are plausible, and that complete dissociation to create three adsorbed oxygen atoms is the most exothermic reaction. We anticipate that the relative instability and entropic inaccessibility of intact ozone adsorption suggests the likelihood of immediate dissociation upon adsorption, so that the actual outcome will depend critically upon the detailed adsorption trajectory. Molecular-dynamics simulations provide the necessary tool kit to determine the most likely reaction products and allow us to discuss the dissociation pathways. We are aware that the limited number of trajectories ($\approx$20) studied in the present work falls well short of strict statistical significance but believe nevertheless

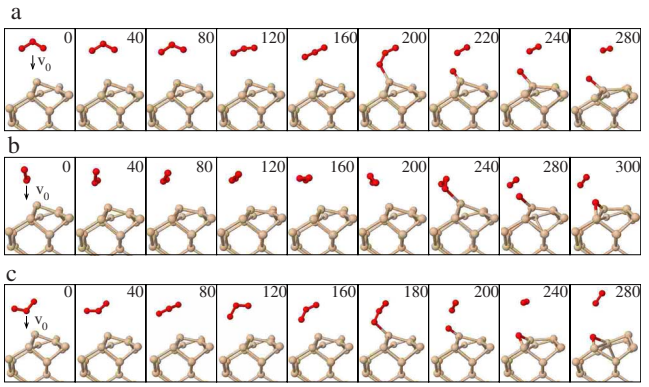

FIG. 5. (Color online) Molecular-dynamics trajectories for O_3 approaching Si^u. Time evolution given in femtosecond.

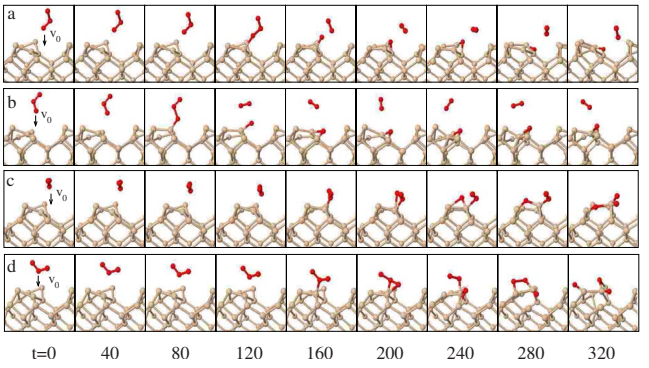

FIG. 6. (Color online) (a)–(d) Molecular-dynamics trajectories for O_3 approaching Si^d. Time evolution given in femtosecond.

that our simulations essentially reflect the dominant processes.

The trajectories observed in this study can be classified into two distinct interaction types: interaction with the up Si-dimer atom (Si^u) or interaction with the down Si-dimer atom (Si^d), of which representative trajectories are presented below. Aiming the molecule at the trough between the dimer rows shows little interaction initially, until ozone gets close enough to the surface, where it is eventually attracted toward either a neighboring Si^u or Si^d reaction site. No direct reaction with a subsurface Si atom is observed, instead trajectories similar to those described below occur.

1. Above Si^u

Three typical reaction pathways for the first interaction type, where O_3 has been placed in three distinct starting orientations above the up Si-dimer atom (Si^u), are shown in Fig. 5. In (a) the ozone molecule is initially oriented with its terminal oxygen atoms pointing downward, within a plane containing the DB, and with its initial velocity directed vertically at the surface. Over the course of 160 fs the molecule is steered by interaction with Si^u and rotates into an orientation in which the shortest Si-O vector (by now around 3 Å in length) lies almost perpendicular to the molecular plane. After $t=200$ fs, the closest oxygen atom accelerates toward Si^u and initiates the dissociation process. During this acceleration, the other two oxygen atoms barely move. After $t=220$ fs, the extended O-O bond breaks; the resulting O_2 molecule drops into its triplet ground state and is repelled from the surface.[32] The binding O atom attaches to Si^u and pushes it into the surface. In the time frame of 240–280 fs we observe a full Si-O vibrational cycle, during which the Si dimer adopts a more horizontal geometry. In our extended molecular-dynamics calculations, this Si-O adsorption site remains stable, while the vibrational energy is gradually dissipated into the substrate.

In (b) the ozone molecule is initially oriented with terminal oxygen atoms pointing upward and its plane rotated 90° about the surface normal compared to the case above. The central O atom, which is now closest to the surface, is repelled by Si^u and the molecule rotates over a period of 200 fs into an orientation where a terminal O atom gets close to Si^u and the shortest Si-O vector lies nearly perpendicular to the molecular plane. After $t=240$ fs, the terminal O and Si^u atoms are accelerated toward each other, initiating the dissociation. After t=280 fs, the extended O-O bond is broken and O_2 is formed; the latter relaxing into its spin triplet configuration and ultimately departing from the surface. The adsorbed O atom retains significant kinetic energy. Since its velocity vector is not aligned with the dimer axis (280 fs), the O atom is incorporated into the Si backbond (300 fs). The dimer becomes momentarily flat and then flips into its opposite tilt, so the adsorbed O atom eventually occupies the more favorable lBB site (not shown in Fig. 5).

In (c) ozone is initially oriented with terminal oxygen atoms pointing upward, within a plane containing the DB. Again the central O atom is repelled by Si^u and the molecule rotates during 120 fs into a more favorable orientation similar to those described above. The terminal O atom is accelerated toward Si^u and at $t=180$ fs the dissociation process starts. As observed in (b), the adsorbed O atom breaks the Si backbond and O_2, now in its triplet configuration, desorbs from the surface. After t=280 fs, we again observe a flip of the Si dimer, as the O atom, which is originally incorporated into the uBB, prefers to occupy the more stable lBB.

2. Above Si^d

In Fig. 6 we show four characteristic trajectories[33] of the second interaction type, where O_3 is placed above the down Si-dimer atom Si^d.

In trajectories (a) and (b) the ozone molecule approaches Si^d with one terminal O atom closest. The molecule moves toward the surface with little steering interaction; whereas Si^d is attracted toward the incoming O_3, lifting the Si dimer into a more symmetric geometry. After about $t=120$ fs the shortest Si-O distance is about 2.1 Å for both trajectories. At this time step the ozone molecule is already significantly deformed. The O-O distance between the central O and the outward-pointing O atom has contracted to about 1.2 Å, whereas the distance to the surface-directed O atom has stretched toward 1.55 Å. After $t=160$ fs the stretched O-O bond is finally broken and there remains one O atom binding to the Si^d site.

In (a), between 200 and 240 fs, we observe the diffusion of the adsorbed O atom to a neighboring dimer within the

same row, where it incorporates into the Si-Si uBB. After $t=320$ fs the dimer has flipped and the O atom occupies the more stable lower backbond site. The released O_2 molecule floats toward the opposite Si^u, approaching it as close as 2.8 Å, before it is eventually repelled and desorbs from the surface.

In (b) the binding O atom breaks the lower Si backbond. The resulting kinetic energy causes intense vibrations, pushing the Si^d atom into the substrate. The thermal energy is gradually transferred onto the neighboring atoms and all bonds stay intact. The recoil of the O_2 molecule is directed away from the surface and again the gas phase O_2 does not react with the Si surface.

Trajectories (c) and (d) show a very different reaction product. Initially, the ozone molecule approaches Si^d with its central O atom closest and we observe little surface-induced steering by Si^d. Instead, after around $t=160$ fs, the central O atom binds with Si^d and initiates the dissociation process. While the central O atom is vibrating at a Si-O distance of about 1.7 Å, one of the terminal O atoms also gets close to Si^d. The O-O bond is stretched and eventually breaks, leaving both atomic oxygen and molecular O_2 bonded to the same Si atom. Just 40 fs later, the chemisorbed O_2 has dissociated too. In trajectory (c) the Si^u of the neighboring dimer binds to the dangling O atom of the O_2 molecule and initiates its dissociation. The two resulting O atoms each bind to a separate Si^u atom, whereas in trajectory (d) O_2 dissociates by reacting entirely on a single dimer. Even here, the reaction extends to the neighboring dimer as one O atom bridges to the adjacent Si^u. Reflecting the highly exothermic nature of the complete dissociation, we observe in snapshots 280 and 320 fs of trajectory (d) a bond breaking between the subsurface Si atom and the O atom incorporated originally into the backbone. At least in this trajectory the bond breaking is only of temporary nature and on a longer time scale ($\approx$600 fs) does not lead to any surface restructuring.[34]

C. Electronic structure

Having observed that ozone interacts quite differently with the two surface sites Si^u and Si^d, we carry out a combined energetic, structural, and electronic structure analysis during the observed pathways in order to explain the distinct pattern.

Without loss of generality we have picked the trajectory depicted in Fig. 5(a) as our model for interaction with Si^u and that depicted in Fig. 6(d) for interaction involving Si^d and represent detailed information for each in Figs. 7 and 8, respectively. First, we show the potential-energy evolution during these trajectories. As the total energy during our molecular-dynamics simulations is conserved, any decrease in the potential energy relates directly to an increase in the kinetic energy. Then we depict the bond-length evolution between the intramolecular O atoms and the distance between the Si and O atoms which are about to interact. The initial rate of drop in bond length relates to the speed at which the two atoms approach each other, while oscillations relate to the onset of phonon vibrations. Finally, we obtain information about the electronic structure by looking at the evolution of the integrated spin densities, and visualize spin densities and electron-density differences of key intermediate structures. The net spin density $s(\mathbf{r})$ is defined as the electron-density difference between spin-up and spin-down electrons $[s(\mathbf{r})=\rho_{\uparrow}(\mathbf{r})-\rho_{\downarrow}(\mathbf{r})]$. If integrated over its spatial coordinates, we obtain two useful measures of the total spin of the system $S=\int s(\mathbf{r})d\mathbf{r}$ and $\bar{S}=\int|s(\mathbf{r})|d\mathbf{r}$. Only if $\bar{S}$ is zero can one treat the system as spin unpolarized. Both S and $\bar{S}$ may vary during the course of a reaction, since neither is a conserved quantity in an extended system.

The interaction of O_3 with Si^u (Fig. 7) can be classified into three reaction stages. In reaction stage I, ozone is at a high distance above the surface (>3.5 Å). The potential-energy surface is fairly flat, indicating that there is only a weak interaction between the surface and the molecule. The distance between the closest silicon surface atom Si^u and the oxygen atom O^3, to which it will eventually bond, decreases gradually with ozone's initial velocity directed toward the surface. Ozone's internal bond lengths vibrate gently around their equilibrium distance of 1.3 Å in a symmetric fashion, which gives small oscillations in the potential energy. The isosurface of $s(\mathbf{r})$ in snapshot (i) reveals a small electron transfer into the O_3 LUMO, which gives an electronic structure that is by 0.25 eV more stable relative to a gas phase ozone and clean surface. The majority spin in this orbital is gradually, by snapshot (ii), counterbalanced by a spin density of opposite sign located on the Si^u site and on ozone's HOMO, which is due to electron depletion. As the reaction enters stage II (Si-O bond formation and O-O_2 bond breaking) the potential energy drops from its initial plateau by 0.14 eV to a slightly lower plateau. The shortest Si-O distance begins to decrease more rapidly, highlighting a growing attractive force. In addition, the integrated spin S and $\bar{S}$ have both become zero, which is indicative of the onset of covalent bonding. Indeed, we observe that the electron-density difference plot, inset (iii) $\Delta\rho(\mathbf{r})$, reveals an increasing interaction between one terminal O atom and the Si^u. Electrons are transferred from the Si^u dangling bond and the O_3 HOMO into the O_3 LUMO. This electron accumulation, however, is not shared equally between the O atoms; instead it is more concentrated on the terminal O atoms, and most of all on the O atom in close proximity to Si^u. In the transition region from stages II to III, the potential energy begins to decline steeply. In snapshot (iv) the energy has already dropped (without exhibiting any activation barrier) by roughly 1 eV relative to its previous plateau. The bond length between the reacting terminal O and the central O atom starts to increase while the distance between this terminal O and Si^u atom decreases further. The spin densities reveal a deformation of the LUMO orbital; the π coupling of the binding terminal O atom with the O_3 LUMO is decreased, while the σ coupling with the Si^u dangling bond emerges. The transition to the final stage III is sharp and highlighted by an abrupt change in the integrated spin S. The dissociation of O_3 into an O atom on the surface and gas phase O_2 is completed; O_2 has relaxed into its spin triplet configuration, which consists of electrons with parallel spin occupying the π_x and π_y orbitals [O_2's singly occupied MOs (SOMOs)]. While O_2 gradually desorbs from the surface, its weak spin interaction

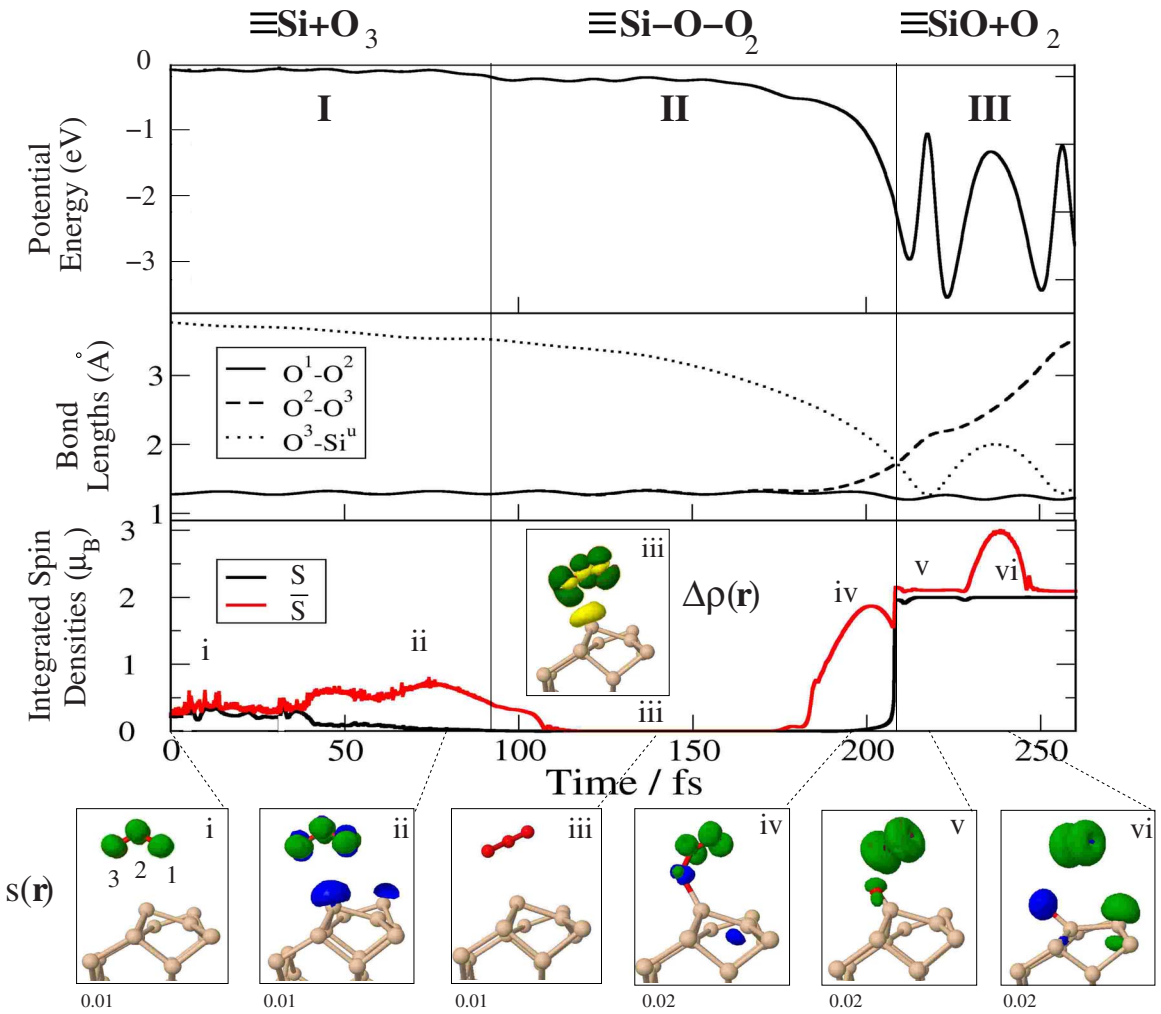

FIG. 7. (Color online) Analysis of the trajectory depicted in Fig. 5(a). Snapshots of the electronic structure are marked as i–vi with isosurfaces of the net spin densities at either 0.01 or $0.02\mu_B$ Å^{-3} [marked $s(\boldsymbol{r})$]. For visualization purposes we have chosen green (gray tone in snapshot i) to mark the regions of majority spin at time zero and kept this assignment throughout the trajectory. Inset (iii) [marked "$\Delta\rho(\mathbf{r})$"] shows an electron-density difference plot with a threshold of $0.01e$Å^{-3} [green (dark) highlighting electron accumulation and yellow (light) electron depletion].

with the surface O atom, as shown in snapshot (v), diminishes. In snapshot (vi) we observe an interesting aftereffect in this reaction. As the surface O atom has received a large part of the released heat of adsorption, the Si-O bond exhibits large vibrations, which are gradually dissipated into the surface, and leads the surface dimer to briefly sample a horizontal position. When the dimer achieves this horizontal position and the Si-O distance is at its maximum, we observe a surface singlet biradical, which is defined as featuring two unpaired electrons of opposite spin: one electron occupies the O p orbital while the other electron occupies the dangling bond of the nonbinding Si atom (N.B.: this biradical is by 0.05 eV more stable compared to an unpolarized calculation and a Mulliken population analysis reveals spin densities in the order of $0.5\mu_B$ localized on each site).

In Fig. 8 we show the corresponding analysis of O_3 approaching Si^d with its central O atom closest. This reaction, which eventually leads to a complete dissociation, can be classified into four stages. In stage I, the potential-energy surface is fairly flat and O_3 interacts only weakly with the surface. Electrons from Si^u sites are donated into the O_3 LUMO. In snapshot (i) we observe spin-polarized electron densities localized on the molecule only; but as ozone gets closer and the electron transfer increases, we find electron densities of opposite spin polarization localized on the two nearest Si^u dangling bonds. Note that this electron transfer is observed for both type of reactions with Si^u and with Si^d; in the early stage of the reaction Si^d shows no interaction with the incoming molecule. Si^u atoms from the neighboring dimer row (not shown in the insets) are not involved in this electron transfer. Stage II involves the docking between the central O atom and Si^d. The potential energy drops by 0.75 eV to a plateau with Si^d-O^2 vibrations, during which the ozone molecule reorients. The integrated spin polarization $\bar{S}$ has reached its maximum of around $2\mu_B$ by snapshot (iii), which is more than twice the value observed in the interaction with Si^u (see Fig. 7). In stage III, the first dissociation takes place and O_3 breaks into an O atom and O_2: both adsorbed to the surface. $\bar{S}$ has dropped to zero by snapshot (iv), which is indicative of the onset of covalent bonding.

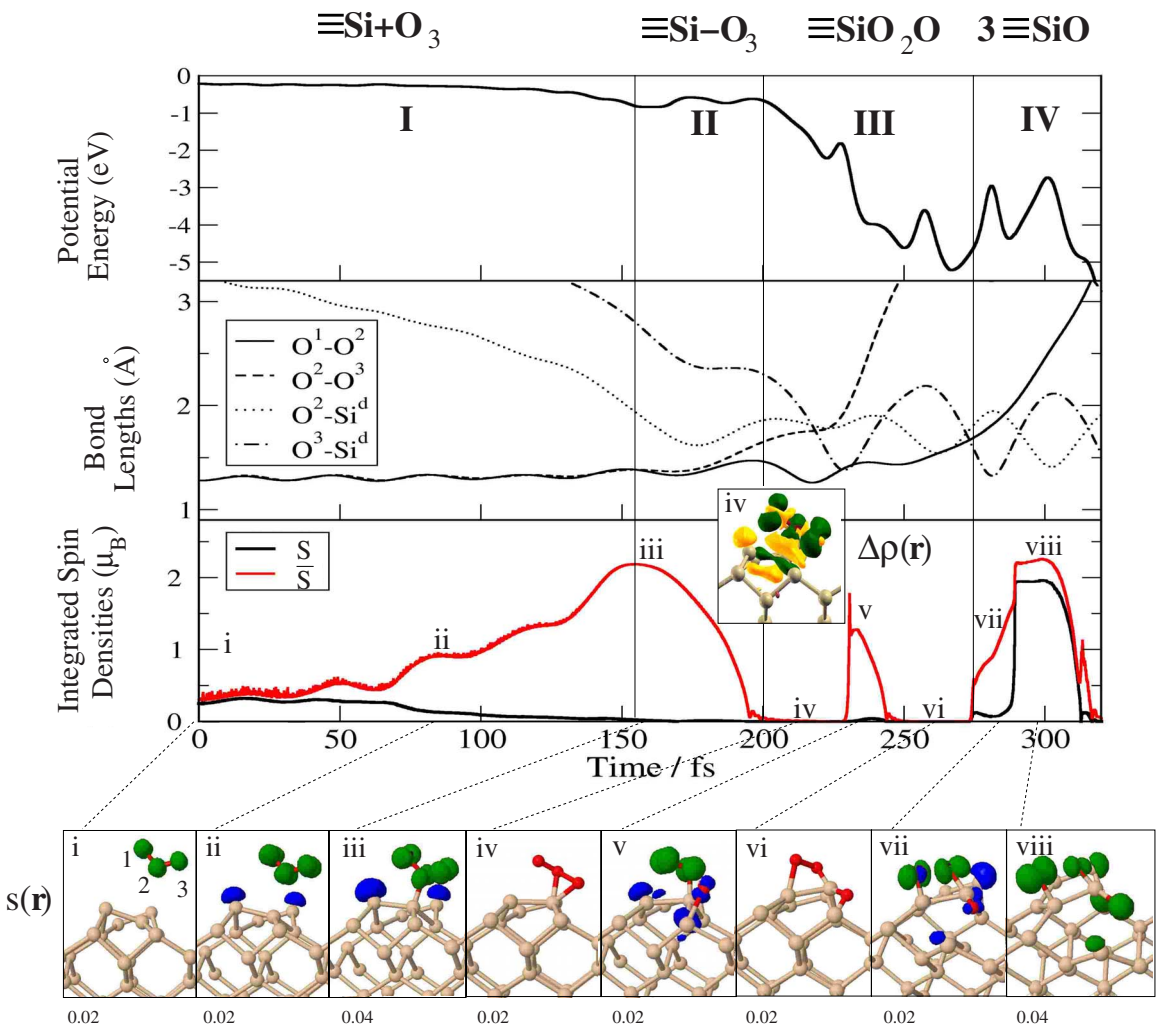

FIG. 8. (Color online) Analysis of the trajectory depicted in Fig. 6(d). Snapshots of the electronic structure are marked as i–viii with isosurfaces of the net spin densities at either 0.02 or $0.04\mu_B$ Å^{-3}. For visualization purposes we have chosen green (gray tone in snapshot i) to mark the regions of majority spin at time zero and kept this assignment throughout the trajectory. Inset (iv) [marked "$\Delta\rho(\mathbf{r})$"] shows an electron-density difference plot at an isosurface threshold of $0.02e$Å^{-3} [green (dark) highlighting electron accumulation and yellow (light) electron depletion].

The Si dimer has been lifted into a horizontal geometry, while two O atoms bind to the same Si-dimer atom. A visualization of the electron transfer reveals a more complex behavior than for the Si^u reaction. Electron accumulation is localized in the O_3 LUMO and in the Si-Si bonds surrounding Si^d, whereas electron depletion is highly localized above Si^u and more delocalized above Si^d and in the region below the DB.

Snapshot (v) depicts the instance when the released O atom is about to break the Si-Si backbond, while O_2 is bound via one atom to its Si atom. The integrated spin density $\bar{S}$ experiences a temporary peak, as one of O_2 π electrons becomes unpaired, while the other forms the Si-O bond. The surface counterbalances this spin polarization with opposite spin densities localized at Si^u and Si^d, which results in a value of zero for S. In snapshot (vi) the O_2 molecule is chemisorbed to the DB, saturating any unpaired electrons, and O is incorporated into the BB, while the dimer has flipped into an asymmetric structure opposite to its original tilt. This intermediate structure resembles the most stable "O(a)+O_2(a)" optimized structure discussed in Fig. 2. Our static calculations show that this adsorption structure upon equilibration would release a heat of adsorption of 8.66 eV. This large energy release allows the system to overcome any activation barrier and relax into a more stable reaction product. Thus, in our MD simulations a partially dissociated but fully adsorbed structure ["O(a)+O_2(a)"] appears only as a short-lived reaction intermediate before full dissociation ["3O(a)"].

In the final stage IV, O_2 dissociates, and we have three highly energetic O atoms on the surface. The total kinetic energy oscillates in the range of 3–5 eV. These energy oscillations relate to snapshots (vii) and (viii), where the Si-O backbond is temporarily broken and unpaired electrons result in spin densities of around $2\mu_B$. The surface O atoms are high in kinetic energy, enabling diffusion to neighboring sites, while their heat is gradually dissipated into the substrate.

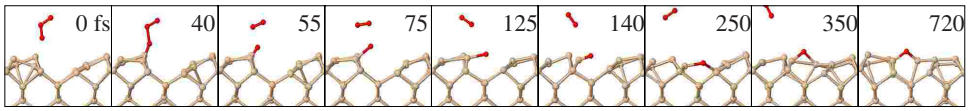

FIG. 9. (Color online) Molecular-dynamics trajectory of O_3 on hot surface. Silicon dimer bond breaks and oxygen forms a Si-O-Si bridge between dimer rows. Time evolution given in femtosecond.

The differences between the docking geometries on Si^u and Si^d, which lead to the two different reaction outcomes, are investigated. In the interaction with Si^u only ozone's binding terminal O is in the vicinity of a surface atom [in the docking geometry depicted in Fig. 7 (iv) the Si-O distance is 2.0 Å and continues to decrease], while the other two O atoms are more than 3.2 Å distant from the nearest surface atom Si^u and more than 4.5 Å distant from the second-nearest surface atom Si^d. In contrast, in the interaction with Si^d in addition to the central O, which exhibits a Si-O distance of around 2.0 Å, both terminal O atoms are near enough to Si surface atoms to react further. In the docking geometry depicted in Fig. 8 (iv) one terminal O is 2.3 Å distant from Si^d, while the other terminal O is 2.8 Å. Both distances drop as ozone dissociates and the Si atoms obtain these oxygen atoms as bonding partners.

IV. DISCUSSION

In contrast to the variety of reaction products suggested by static calculations, molecular-dynamics simulations reveal two dominant reaction pathways, which proceed without any activation barrier. Ozone either partially dissociates into an oxygen adatom, which originally binds to a Si-dimer atom in the on top configuration Si^u, before being incorporated[35] into a binding site on the dimer (lBB or DB), and in a desorbing molecular oxygen; or it fully dissociates into three oxygen adatoms, which are also eventually incorporated into the Si surface top layer. The active reaction sites for the dissociation are the two Si-dimer atoms Si^u and Si^d, which exhibit differing interactions with ozone. Whereas Si^u favors interaction with a single terminal O atom, the Si^d is able to interact with both terminal and central O atoms. A direct full dissociation is only observed when the central O atom of ozone interacts with Si^d. Yoshinobu[36] argued that the electron rich Si^u atom ought to act as a Lewis base, while the electron deficient Si^d atom should be a Lewis acid. The electrophilic ozone molecule, as a Lewis acid, can therefore be expected to react most strongly with Si^u; but in fact this interaction is if anything too rapid to allow full dissociation to occur and instead leads only to partial dissociation.

We also observe that the initial velocity of the O_3 molecule has little influence[37] on the reaction itself. Instead, either of the two surface sites Si^u or Si^d determines the reaction pathway. The Si^u site exhibits a large steering effect on the incoming ozone molecule by repelling the central O atom and attracting either of the two terminal O atoms. In this interaction, we observe a single docking geometry, where one of the terminal oxygen atoms binds to Si^u to maximize the overlap between the surface dangling bond and the O_3 LUMO. This initiates the dissociation of O_3 into a single oxygen adatom, initially binding to Si^u, and a gas phase O_2 desorbing from the surface. In the majority of trajectories, the absorbed O atom stays in this Si^u binding site only for a short time, as it has sufficient kinetic energy to break the neighboring DB or uBB directly. If incorporated into the uBB the Si-dimer flips, so the O atom is able to relax into the more stable lBB site. In contrast, the alternative reactive surface site Si^d does not exhibit this steering effect. Depending on its initial orientation, O_3 docks either with its terminal or central O atom to Si^d. If a terminal O atom binds to Si^d, a partial dissociation as described for the Si^u site takes place and atomic O is directly incorporated into the lBB site. When the central O atom approaches Si^d, O_3 dissociates first into O and O_2—both binding to Si^d—and then subsequently O_2 dissociates into two O adatoms. This complete dissociation into three adsorbed O atoms releases kinetic energy of up to 5 eV in the time frame of our MD calculations, causing O atoms to diffuse to neighboring dimers, while adjacent Si-Si or Si-O bonds break temporarily. On a longer time frame, as our static calculations have shown, a complete dissociation where three O adatoms are incorporated into Si-Si bonds would equilibrate to a heat of adsorption higher than 11 eV.

STM studies[14,15] on the initial oxidation of Si{001} by ozone revealed features believed to correspond to single O adatoms. The most common adsorption sites for the O adatom were assigned to either the dimer or backbond sites, which coincide with the most common adsorption sites found during partial dissociation in our MD simulations. Itoh *et al.*[14] also determined, however, a smaller amount of alternative adsorption sites located not on the dimer itself but between two dimer rows (the ratio of which was estimated to be 1:10 compared to adsorption in the dimer bond).

Indeed, a candidate for such a structure was found in one of our MD simulations where the surface was given an initial temperature. In the trajectory depicted in Fig. 9 the ozone was placed ≈3 Å above Si^d with an initial velocity of 5 Å ps^{-1} (t=0 fs). These initial conditions are equivalent to the trajectory shown in Fig. 6(b), except that the surface here has been prepared to have a temperature of ≈400 K. During the equilibration phase prior to the introduction of the ozone, the reconstruction of the surface changed from its original p(2×2) state, as one of the Si dimers flipped. This leaves antiparallel dimers in one row and parallel dimers in the other. As discussed before, ozone reacts with Si^d through its closest terminal O atom (40 fs) to give an O adatom and gas phase O_2 (55 fs). In contrast to the previous trajectory, the O adatom is not incorporated into the BB but stays adsorbed on the dimer atom and exhibits strong Si-O stretch vibrations (75 fs), which become the motor for the following surface restructuring. As the Si-O vibrations are in opposite direction to the Si-Si dimer bond, the DB is stretched (125 fs) and eventually breaks (140 fs). This leaves one Si-dimer atom

with two dangling bonds, while the Si-O complex, still exhibiting heavy Si-O vibrations, approaches the opposite dimer row within ≈100 fs. Eventually the O atom binds to a second-layer Si atom, which forms a Si-O-Si bridge across the trough (250 fs). This second-layer Si atom is lifted upward, which breaks one of its subsurface Si-Si bonds (350 fs). The Si atom with the two dangling bonds gets closer to its previous binding partner and temporarily forms the dimer bond again (720 fs). For the continuation of the simulation (≈1 ps) the oxygen stays in this bridge position. A structure optimization confirms that this is indeed a stable structure. For the partial dissociation of ozone, it releases a heat of adsorption of 3.65 eV. It is by 0.79 eV less stable than the bridging site where the O atom binds between the two second-layer atoms across the trough.[38] We conclude that this bridging structure could be either the structure observed in the STM study or alternatively an intermediate structure, before the O atom diffuses into a more stable bridging site.

The STM results suggest that a complete dissociation (as seen in some of our MD simulations) is either a rare event masked by oxygen diffusion or related to the observed increase in defect sites. This increase in defect sites during ozone exposure was interpreted as being related to the formation of volatile SiO, also referred to as etching in the literature. Due to the limitations of first-principles MD in terms of the number of trajectories and time scales, we did not observe any direct etching event.

Nevertheless, based on energetics, we can reasonably ask whether a complete dissociation increases the likelihood of an etching event. There are two aspects to consider: the heat of adsorption released and the activation barrier to overcome. First, the total heat of adsorption of a complete dissociation of ozone is very large. Nevertheless, this released energy is not focused into a single O atom but shared between three O atoms. Second, as Hemeryck *et al.*[39] showed, the activation barrier for etching has a strong dependency on the oxidation state of the Si atom. The barrier for etching of a singly oxidized Si atom Si^{1+} was found by those authors to be much lower (≈2 eV) than for higher oxidized Si atoms (Si^{2+}, Si^{3+}, and Si^{4+}). So unless the O adatoms diffuse to distant sites to form Si^{1+}, SiO ejection due to complete ozone dissociation would need to overcome a high barrier. In our simulations, we observe O adatom diffusion and Si-Si bond breaking but do not see any SiO ejection. In contrast, for a partial dissociation where only a single O atom is deposited onto the surface, the heat released is initially concentrated only on the binding Si^{1+} and on the O atom. This kinetic energy is close to the 2 eV necessary for SiO ejection and so increases the probability for an early etching event.

In contrast to O_2, which was found to dissociate only over the Si^d site,[40] we find that O_3 easily reacts with both Si^u and Si^d sites, which opens a wide barrierless dissociation channel.

V. CONCLUSION

We conclude that O_3 on Si{001} is highly reactive and exhibits an initial sticking probability close to unity. Two dominant reaction pathways are observed in our molecular-dynamics simulations: either O_3 dissociates into a single O adatom and gas phase O_2 (partial dissociation) or it dissociates fully into three O adatoms (complete dissociation). The dissociation proceeds without any activation barrier and involves one of two possible surface reaction centers: the electrophilic ozone reacts with either the electron rich Si^u or the electron deficient Si^d atom. The more reactive up dimer atom Si^u displays a pronounced steering effect onto the incoming molecule, where Si^u maximizes the O_3 LUMO overlap with a terminal O atom before ripping it off. In contrast, the less reactive down dimer atom Si^d does not exhibit this steering effect and is able to react also with the central O atom, which results in a dissociation of the whole molecule. Paradoxically, the surface site that initially interacts least strongly with ozone is the one that is capable of dissociating the molecule completely. The reaction is highly exothermic and releases a heat of adsorption of up to 5.14 and 13.51 eV for the partial and complete dissociation, respectively. It is expected that the resulting hot O adatoms are responsible for the experimentally observed SiO ejection. In the early oxidation stage, no direct O insertion into the trough region is observed, although O adatoms can diffuse from their original dimer adsorption site into the trough.

ACKNOWLEDGMENTS

We thank K. Nakamura for fruitful discussions. S.J.J. is a Royal Society University Research Fellow and C.K.F. is supported by a studentship from The Leverhulme Trust.

*Corresponding author; sjj24@cam.ac.uk

[1] T. Engel, Surf. Sci. Rep. **18**, 93 (1993).
[2] M. L. Green, E. P. Gusev, R. Degraeve, and E. L. Garfunkel, J. Appl. Phys. **90**, 2057 (2001).
[3] K. Hirose, H. Nohira, K. Azuma, and T. Hattori, Prog. Surf. Sci. **82**, 3 (2007).
[4] S. Ichimura, H. Nonaka, Y. Morikawa, T. Noyori, T. Nishiguchi, and M. Kekura, J. Vac. Sci. Technol. A **22**, 1410 (2004).
[5] K. Koike, T. Fukuda, S. Ichimura, and A. Kurokawa, Rev. Sci. Instrum. **71**, 4182 (2000).
[6] S. Chao, R. Pitchai, and Y. Lee, J. Electrochem. Soc. **136**, 2751 (1989).
[7] A. Kazor and I. W. Boyd, Appl. Phys. Lett. **63**, 2517 (1993).
[8] S. Hosokawa and S. Ichimura, Rev. Sci. Instrum. **62**, 1614 (1991).
[9] K. Nakamura and S. Ichimura, Jpn. J. Appl. Phys., Part 1 **44**, 7602 (2005).
[10] A. Kurokawa, K. Nakamura, S. Ichimura, and D. W. Moon, Appl. Phys. Lett. **76**, 493 (2000).
[11] H. S. Chang, S. M. Choi, D. W. Moon, and H. Hwang, Jpn. J. Appl. Phys., Part 1 **41**, 5971 (2002).
[12] N. Kameda, N. Nishiguchi, Y. Morikawa, M. Kekura, H.

Nonaka, and S. Ichimura, J. Electrochem. Soc. **154**, H769 (2007).
[13] K. Nakamura, A. Kurokawa, and S. Ichimura, Jpn. J. Appl. Phys., Part 2 **39**, L357 (2000).
[14] H. Itoh, K. Nakamura, A. Kurokawa, and S. Ichimura, Surf. Sci. **482-485**, 114 (2001).
[15] T. Narushima, M. Kitajima, A. N. Itakura, A. Kurokawa, S. Ichimura, and K. Miki, Surf. Sci. **601**, 1384 (2007).
[16] C. K. Fink and S. J. Jenkins, Surf. Sci. Lett. **602**, L100 (2008).
[17] T. Nishiguchi, Y. Morikawa, M. Miyamoto, H. Nonaka, and S. Ichimura, Appl. Phys. Lett. **79**, 382 (2001).
[18] Z. J. Cui, J. M. Madsen, and C. G. Takoudis, J. Appl. Phys. **87**, 8181 (2000).
[19] M. D. Segall, P. J. D. Lindan, M. J. Probert, C. J. Pickard, P. J. Hasnip, S. J. Clark, and M. C. Payne, J. Phys.: Condens. Matter **14**, 2717 (2002).
[20] J. P. Perdew, J. A. Chevary, S. H. Vosko, K. A. Jackson, M. R. Pederson, D. J. Singh, and C. Fiolhais, Phys. Rev. B **46**, 6671 (1992).
[21] D. Vanderbilt, Phys. Rev. B **41**, 7892 (1990).
[22] H. J. Monkhorst and J. D. Pack, Phys. Rev. B **13**, 5188 (1976).
[23] T. H. Fischer and J. Almlof, J. Phys. Chem. **96**, 9768 (1992).
[24] M. D. Segall, R. Shah, C. J. Pickard, and M. C. Payne, Phys. Rev. B **54**, 16317 (1996).
[25] In contrast to an NVT ensemble our system does not exchange heat with a thermal bath, instead the total energy is conserved, which enables us to investigate the energy transfer during these exothermic reactions. Introducing a thermostat would, in effect, introduce instantaneous cooling of the reaction, whereas for a semiconductor surface we expect heat transfer away from the adsorption site should occur primarily via phonon excitation and on a relatively long time scale.
[26] For example, looking at the complete dissociation, a 0.75 ML O adatom coverage, corresponding to 3 O atoms in a (2×2) unit cell, is by 0.07 eV per O atom less stable than a coverage of 0.19 ML O adatoms, corresponding to 3 O atoms in a (4×4) unit cell.
[27] T. Uchiyama and M. Tsukada, Phys. Rev. B **53**, 7917 (1996).
[28] On performing convergence tests with a higher k-point density $(3\times3\times1$ and $4\times4\times1)$, we reproduced the same trend in stability and obtained heats of adsorption for the lBB, DB, and Si^u sites of 5.24, 5.04, and 4.15 eV, respectively.
[29] The physical origin that a complete dissociation is the most stable reaction product can be viewed in terms of balancing the energy costs for splitting the O-O and Si-Si bonds with the energy gains for forming the Si-O bonds. Our calculations show that to split off a single gas phase O atom from the O_3 costs 1.44 eV, whereas to split the remaining O_2 costs a further 5.68 eV. Thus, a complete dissocation of ozone would cost 7.12 eV. On the other hand, the adsorption of a single O atom or three single O atoms, enables the formation of two or six Si-O bonds, respectively. Since the energy of Si-O bonds, however, varies dependent on structure, and since Si-Si bond are also broken, DFT calculations are crucial in understanding and determining the actual stability of each structure.
[30] In this adsorption site, the O atom bridges two Si atoms from neighboring dimers along the dimer row.
[31] K. Kato, T. Yamasaki, and T. Uda, Phys. Rev. B **73**, 073302 (2006).
[32] Depending on its recoil, we found trajectories where the gas phase O_2, instead of desorbing, reacted with the Si^d of the opposite row and dissociated in a way described by Ciacchi *et al.* (Ref. 40).
[33] Except for (a), where we used a (2×2) cell, we enlarged our surface cell in (b), (c), and (d) to a unit cell of (4×2) size, which includes two rows with two dimers each. Accordingly, we have adapted the **k**-point sampling for the (4×2) supercell to a Monkhorst-Pack grid of $1\times2\times1$ dimensions. For visualization purposes we show figure (a) also as a (4×2) surface cell, by including periodic image atoms. The larger cells were necessitated by trajectories involving multiple adsorbed atoms spread across the simulation cell.
[34] To study how the highly exothermic complete dissociation affects the surface oxidation, longer time scales, surface temperature, and a larger unit cell would have to be considered, which is beyond the scope of this work.
[35] The activation barriers for O diffusion from Si^u to DB and lBB sites have been calculated by Hemeryck *et al.* (Ref. 38) to be 0.11 and 0.38 eV, respectively. Due to the large heat of adsorption released during the dissociation, the O adatom on the Si^u diffuses easily into the more stable DB or lBB sites.
[36] J. Yoshinobu, Prog. Surf. Sci. **77**, 37 (2004).
[37] Ozone molecules with velocities ranging from 400–800 m/s gave the same qualitative reaction outcome.
[38] A. Hemeryck, N. Richard, A. Esteve, and M. D. Rouhani, Surf. Sci. **601**, 2339 (2007).
[39] A. Hemeryck, N. Richard, A. Esteve, and M. D. Rouhani, Surf. Sci. **601**, 2082 (2007).
[40] L. C. Ciacchi and M. C. Payne, Phys. Rev. Lett. **95**, 196101 (2005).